Applied Ocean Research 40 (2013) 74–82

Contents lists available at SciVerse ScienceDirect

Applied Ocean Research

journal homepage: www.elsevier.com/locate/apor

Prediction of offshore bar-shape parameters resulted by cross-shore sediment transport using neural network

Murat İhsan Kömürcü[a,*], Mehmet Aydın Kömür[b], Adem Akpınar[c], İsmail Hakkı Özölçer[d], Ömer Yüksek[a]

[a] Karadeniz Technical University, Civil Engineering Department, 61080 Trabzon, Turkey
[b] Aksaray University, Civil Engineering Department, 68100 Aksaray, Turkey
[c] Gümüşhane University, Civil Engineering Department, 29000 Gümüşhane, Turkey
[d] Zonguldak Karaelmas University, Civil Engineering Department, 67100 Zonguldak, Turkey

ARTICLE INFO

Article history:
Received 15 May 2012
Received in revised form 11 January 2013
Accepted 18 January 2013

Keywords:
Coastal profiles
Neural network
Storm-built profiles
Bar characteristics
Experimental study

ABSTRACT

In order to understand the features of coastal zone and to utilize the coastal areas, it is necessary to determine the sediment movement and the resulting transport. Waves, topographic features, and material properties are known as the most important factors affecting the sediment movement and coastal profiles. In this study, by taking into consideration of wave height and period (H_0, T), bed slope (m) and sediment diameter (d_{50}), cross-shore sediment movement was studied in a physical model and various bar-shape parameters of the resultant erosion type profile were determined. Using 80 experimental data which are obtained from physical model studies, a neural network (NN) has been calibrated to predict bar-shape parameters of beach profiles. A sensitivity analysis was firstly carried out to decide data of training and test sets. Four different models, in which the rates of their training and testing set data were 80% and 20%, 70% and 30%, 60% and 40%, 50% and 50% were constituted and their performances were compared. It was determined that the model, in which the rate of its training and testing set data was 80% and 20%, respectively, has the best results. Therefore, a total of 64 experimental data were used as training set and the remainders of the experimental data were used as a testing set for the model. The performance of the NN model was compared with the regression equations developed in a previous study and the equations cited in literature indicating better performance over the equations.

© 2013 Elsevier Ltd. All rights reserved.

1. Introduction

Given a beach profile in which the incoming wave energy is effectively dissipated, various wave conditions may lead to different characteristics of erosion and accumulation in this beach profile. In complex coastal phenomena such as beach erosion, physical modeling is often carried out. In previous studies, it was shown that physical modeling produced better results with respect to those by the prototype model. Conversely, numerical models were not satisfactorily fitting due to the complexity of coastal hydrodynamics and there is still ongoing research on its reliability [1–3]. A literature review including the studies carried out in the past is summarized as follows.

Various researchers engaged in studies cross-shore sediment transport models for a variety of beach profiles. During the studies, new experimental and previous data were compared with previous models in the literature [4–6]. Schoonees and Theron [7] have compared 10 models about cross-shore sediment transport with each other and classified the models as best, acceptable and less suitable. However, it is very important to consider the specific purpose of a model application. Larson and Kraus [8] have studied erosion and accretion profiles proposing equations for bar parameters of beach profiles using experimental data (Table 1). Silvester and Hsu [9] analyzed beach profile parameters by non-linear regression techniques using various experimental data obtained from previous works and proposed equations for the bar parameters (Table 1).

Hsu [10] performed experimental and theoretical studies to determine the geometry of offshore bars and suggested some equations for bar parameters (Table 1). Ruessink et al. [11] have made an attempt to determine long time variations of bar crest position in a beach profile using the remote sensing method. Günaydın and Kabdaşlı [12] studied the characteristics of coastal erosion and bars using a physical model in which the mean diameter of particles of 0.35 and the beach slope of 1/5 under regular and irregular wave conditions. They determined the position of erosion and bar geometry by the definition of the related parameters and obtained model functions using non-linear regression methods. Their results show that the wave types, whether regular or irregular, were not effective in describing the geometric characteristics of coastal erosion.

Investigation on how far sediment particles can go away from the coast or how deep sediment particles can transport from still water level (SWL) (depth of closure), has shown that bed topography,

* Corresponding author. Tel.: +90 462 377 2633; fax: +90 462 325 6682.
E-mail addresses: mkomurcu@ktu.edu.tr, mikomurcu@hotmail.com (M. Kömürcü).

0141-1187/$ - see front matter © 2013 Elsevier Ltd. All rights reserved.
http://dx.doi.org/10.1016/j.apor.2013.01.003

Table 1
The selected some existing equations cited in the literature.

References	Equations	Equation number
Hsu [10]	$X_{be}/L_0 = 1.9 \times \xi_\theta (\xi_\theta = \tan\beta/\sqrt{H_0/L_0}$, Iribarren number)	(1)
Silvester and Hsu [9]	$X_{bc}/L_o = 0.022 + 1.508 \times (H_o/L_o)/\tan\beta + 0.140 \times [(H_o/L_o)/\tan\beta]^2$	(2)
Larson and Kraus [8]	$h_{bc} = 0.66 \times H_b (H_b$ = breaking wave height)	(3)
Hallermeier [13]	$h_{bd} = 2.28 \times H_o - 68.5 \times (H_o^2/gT^2)(X_{bd} = h_{bd}/m)$	(4)
Larson and Kraus [8]	$V_{bv} = 0.088 \times H_o^{2.26} \times w^{-1.46} \times T^{0.55}$	(5)

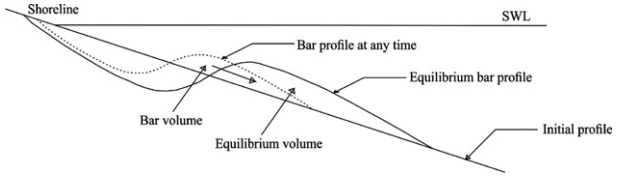


Fig. 1. The equilibrium profile.

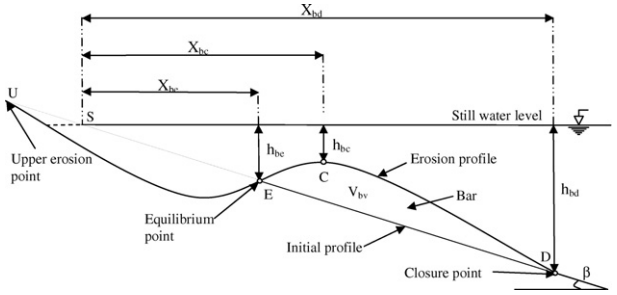


Fig. 2. Selected bar-shape parameters.

sediment particles diameter and wave conditions are influential parameters. An equation for depth of closure was developed [13] (Table 1).

Neural networks are systems that can find complex relationships between any related parameters. In recent years, NNs have been used successfully in various fields of coastal and ocean engineering [14–28].

In this study, the bar-shape parameters of equilibrium beach profiles are studied. A physical model has been set up. The beach slope, the bed material properties and the wave conditions have been modeled, and the bar-shape parameters in the erosion profile are measured. Using experimental data, a neural network (NN) has been calibrated to predict bar-shape parameters of beach profiles. The performance of the NN model calibrated with part of the experimental data is compared to the performance of regression equations and existing equations cited in the literature.

2. Equilibrium profile and bar-shape parameters

A fundamental assumption of beach profile change is the existence of an equilibrium profile to which a beach will tend to achieve equilibrium if exposed to constant wave conditions for a sufficiently long time. The idea is that the beach profile in its equilibrium state dissipates incident wave energy without significant net change in shape [29]. If an equilibrium profile did not exist, the beach would continue either to erode or accrete indefinitely, if exposed to the same wave conditions and with no restrictions in the sand supply. A great difference between initial profile and equilibrium profile for a specific wave climate and grain size implies that a large amount of sand must be redistributed in the process of reaching equilibrium [30].

In considerations of cross-shore sediment transport, it is useful to first examine the case of equilibrium in which there is no net cross-shore sediment transport [31]. As a bar grows, it moves offshore and increases in volume to approach an equilibrium size (Fig. 1). The equilibrium bar volume, however, is not entirely reached in most cases. In such cases, an objective method for determining equilibrium bar volume becomes very important.

In fact, at a micro scale level, the concept of an equilibrium profile is an idealization that cannot be fully achieved in practice, since waves, water level, water temperature, and other conditions cannot be held perfectly fixed. Nevertheless, at a macro scale level, it has been demonstrated that an equilibrium profile can be approached, in which no significant systematic net sand transport occurs, although small perturbations still remain [32].

As a result of interaction between bed topography and parameters of bed material, the beach profile is formed as either an erosion or accumulation profile. In this study, only bar-shape parameters in erosion profile were investigated. These parameters were shown in Fig. 2, in which U, S, E, C, D and β are the upper erosion point, the original beach profile point, the equilibrium point (the initial bar point), the bar crest, the final bar point (depth of closure point) and the angle between initial profile and horizontal line ($\tan\beta$ = m), respectively [33,34]. In Fig. 2, X_{bc} is horizontal distance between the bar crest and original shoreline, h_{bc} is vertical distance between the bar crest and the SWL, X_{be} is horizontal distance between the initial bar point and original shoreline, X_{bd} is horizontal distance between the final bar point and the original shoreline, h_{bd} is vertical distance between the final bar point and SWL, and V_{bv} is the volume of the bar.

3. Laboratory experiments

3.1. Wave flume and measurement system

The experiments were conducted in a wave flume in the Hydraulic Laboratory, Civil Engineering Department, Karadeniz Technical University, Trabzon, Turkey. The wave flume was 33 m long, by 1.4 m wide, by 1.2 m deep. The still water depth was at 0.825 m for 1/10 and 1/15, and at 0.66 m for 1/25 experiments. The wave flume was equipped with a flap-type, impermeable, monochromatic, wavemaker (Fig. 3), and placed parallel to one wall, with a sand beach on the opposite side. Wave records were determined by wave gauges (10 m from the wave paddle) and recorder units [33].

Measured wave heights include the influence of any reflected waves. Reflection coefficients (K_r) were estimated as a function of the surf similarity parameter (ξ), which includes the influence of wave height, period, and beach slope [35]. A widely used predictive equation for K_r is given by [36] as:

$$K_r = \frac{\alpha}{1 + (\beta/\xi^2)} \tag{6}$$

In which α and β are empirically derived, dimensionless coefficients, and ξ is the surf similarity parameter given as $\tan\theta/(H_i/L_o)^{1/2}$

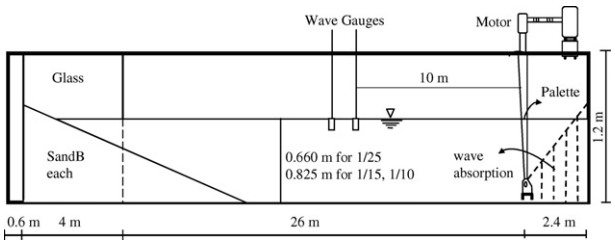


Fig. 3. Wave flume.

[37]. In each case, reflection coefficients in the experiments were estimated to be less than 4.6%. Thus, the measured wave heights were assumed to be equivalent to the incident wave heights.

The flume was divided into seventy sections and each section was sub-divided into three measuring points (i.e., three depths were measured and averaged in a section) and totally 210 points were measured during the experimental studies. A uniform measurement grid of 20 cm × 20 cm was surveyed within the mesh. At each point and time of interest, sand elevations above the basin floor were simply measured [33].

3.2. Experimental variables

A series of laboratory experiments were performed to investigate the variation of coastal profile under different scenarios.The experimental studies were prepared using Froude's model technique under undistorted conditions. The scale of the model was chosen to be 1/25 by taking into account for size of the wave flume (Fig. 3). In the tests, monochromatic waves were used. Many previous researchers noted that simulated beaches evolve differently when subjected to random wave fields as opposed to monochromatic waves with the same basic statistics. With monochromatic waves, the breakpoint location varies less, often leading to a more pronounced sandbar. But, Günaydın and Kabdaşlı [12] showed that the wave types, whether regular or irregular, were not effective in describing the geometric characteristics of the coastal erosion.

Wave conditions were chosen to be between a maximum and minimum to originate the erosion profile, as would be in nature, in order to examine the considered parameters. The deepwater wave heights (H_0) were 6.5, 11.5, 16, 20, 23, 26 and 30 cm for 1.46 s wave period (T), and 6.5, 11.5, 16 and 20 cm for 2.03 s wave period. The initial bed slopes ($m = \tan\beta$) were chosen as 1/10, 1/15 and 1/25.

Determination of material properties in the proposed model was considered as a significant problem. There is no certain method to choose a model on scaling of bed material, although several investigations were carried out recently. On the contrary to that material with different densities are proposed in experimental and theoretical works, there is still an ongoing discussion about this approach [3,38–40]. In this study, four different materials with mean diameters (d_{50}) 0.18, 0.26, 0.33 and 0.40 mm were used with the specific gravity of 2550 kg/m^3. Due to importance of uniformity of grain size distributions of materials, the materials were uniformly distributed in the experimental setup.

There is also a relationship between experiment time and bar-shape parameters. The experiment time was determined by preliminary test for each beach slope until erosion profile reaches the equilibrium. This duration was determined by the criteria which maintain initial bar crest and final bar point fixed, decreasing total moving material quantity below certain ratio and moving materials with the same slope. It was 12 h for 1/10, and 14 h for 1/15 and 1/25 beach slopes. The experimental results used in the present study have been obtained in the study of reference [41]. Besides, in reference [33], regression equations were developed by using the experimental results

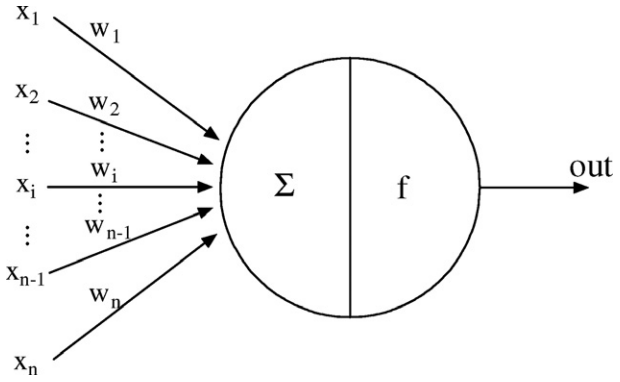


Fig. 4. The structure of an artificial neuron.

obtained in the study of reference [41] and the results of regression equations were compared to the results of equations cited in literature. The best regression equation developed for each bar-shape parameter by reference [33] is presented in Table 2. The experimental results were also evaluated by the genetic algorithms in the study of reference [42]. This study aims to evaluate the experimental results by using neural network.

4. Application of NN to determine bar parameters

4.1. Backgrounds

A neural network (NN) is a computational structure inspired by the study of biological neural processing [43]. NN is a data-modeling tool, which is capable of capturing and representing complex relationships between inputs and outputs. Its instants are composed of large numbers of highly interconnected processing elements that are called as neurons and are tied together with weighted connections. Each neuron works as an independent processing element, and has an associated transfer function, which describes how the weighted sum of its inputs converts the results into an output value. Each hidden or output neuron receives a number of weighted input signals from each of the units of the preceding layer and generates only one output value (Fig. 4). The multilayer perception (MLP) is by far the most well-known and most popular NN among all the existing NN paradigms [44]. It consists of at least three or more layers, and generally it comprises an input layer, an output layer and a number of hidden layers. Each neuron in one layer is connected to the neurons in the next layer and there are no connections among the units of the same layer [45,46]. The number of neurons in each layer may vary depending upon the problem.

The weighted sum of input components is calculated as [47]:

$$y_j = \sum_{i=1}^{n} w_{ij} x_i + \theta_j \tag{12}$$

where y_j is the weighted sum of the jth neuron for the input received from the preceding layer with n neurons, w_{ij} is the weight between the jth neuron and the ith neuron in the preceding layer, x_i is the output of the ith neuron in the preceding layer, θ_j is the bias term of the jth neuron. The output of the jth neuron out_j is calculated with a sigmoid function as follows:

$$out_j = f(y_j) = \frac{1}{1 + e^{-y_j}} \tag{13}$$

The training of the network is accomplished by adjusting the weights and is carried out through a large number of training sets and training cycles (epochs). The goal of the learning procedure is to

Table 2
The best regression equations developed for each bar-shape parameter in the study of Ref. [33].

Equations	Equation number
$X_{be}/L_o = -0.5803 + \exp(0.6508 - 11.471m + 9.0126H_o/L_o + 0.0347H_o/wT)$	(7)
$X_{bc} = -1.9728 + \exp(1.9311 - 13.1274m + 0.2706T + 3.4662H_o - 1008.5d_{50})$	(8)
$h_{bc} = 0.0101m^{-0.6489} \times T^{0.8542} \times H_o^{0.6807} \times d_{50}^{-0.2267}$	(9)
$X_{bd} = 0.7151m^{-0.6804} \times T^{0.5947} \times H_o^{0.4864} \times d_{50}^{-0.1404}$	(10)
$V_{bv} = -0.160 + \exp(-2.1003 - 0.2414m + 0.4698T + 4.3243H_o - 1286.4d_{50})$	(11)

find the optimal set of weights, which in an ideal case would produce the right output for any input. The output of the network is compared with a desired response to produce an error. The performance of the MLP is measured in terms of a desired signal and the criterion for convergence. The performance of training and testing phases were evaluated by means of coefficient of determination (R^2) and mean square error (*MSE*) as follows:

$$R^2 = 1 - \frac{SSE}{\sum_{i=1}^{n}\sum_{j=1}^{k}\left(T_{ij} - \overline{T_{ij}}\right)^2} \tag{14}$$

$$MSE = \frac{SSE}{n.k} \tag{15}$$

where k is the number of neurons in the output layer and n is the number of samples. T_{ij} and out_{ij} are the desired (target) output and output of neural network values, and $\overline{T}_{ij}$ is the average of target outputs. *SSE* is the sum of square of errors, defined as

$$SSE = \sum_{i=1}^{n}\sum_{j=1}^{k}\left(T_{ij} - out_{ij}\right)^2 \tag{16}$$

4.2. The design and training of NN model

An NN model having 4 neurons in input layer, 8 neurons in hidden layer, and 5 neurons in output layer (Fig. 5) was used in the present study. Number of neurons in input and output layers was the number of parameters of input and output of the test. The number of hidden layers and number of neurons in this layer directly affected the performance of network. Since there is no rule of thumb to determine the hidden layer, a trial and error procedure is commonly used to set up the hidden layer [48].

A computer program was written and performed under MATLAB environment. The produced NN model architecture was a multi-layer, feed-forward, and back-propagation architecture. This model was trained using a scaled conjugate gradient training algorithm [48]. A sigmoid function was used as an activation function in the NN model. Therefore, all data were normalized by scaling in a variable between 0 and 1. The maximum value of each parameter was used for the normalization. The number of data points in the training and test sets is important in predicting the best accuracy. In order to determine the best ratio for training and testing sets, several datasets with different ratios are tested for sensitivity. The datasets (training%:testing%) vary from 80:20, 70:30, 60:40, 50:50. Each dataset was trained and tested 20 times and best performances of these experiments are given in Table 3. The best result for prediction accuracy was obtained in the 80:20 ratio tests and therefore it was used in this study.

A total of 80 experimental data were used for training and testing purposes in the NN model. 64 experimental data (80% of all the experimental data) were used for training set and rest of the data for testing set of the model. Table 4 presents all the experiment conditions and scenarios for a total of 80 experimental data. The details relating to bar-shape parameters obtained from the experiments have been given in reference [41]. In this table, the bold experiment numbers represent 16 cases for testing set. On the other words, the 16 cases with the experiment numbers 5, 7, 10, 17, 23, 29, 39, 43, 48, 52, 54, 61, 64, 66, 75, 78 were used for testing set while the other 64 cases were for training set. Number of data and percentage of each parameter value in all the experimental datasets and testing set were also given in Table 4. For choosing data or cases used in testing set or training set the attention was given to representing all of the experimental data. For example, it is seen from Table 5 that for $m = 0.1000$, 0.0667, and 0.040 the numbers of data are 35, 30, and 15 in the all the experimental datasets and their percentages in all the set are 43.7, 37.5, and 18.8, respectively. On the other hand, the cases in testing set have values close to these percentages for each beach slope. This is also valid for the selected values of the other three parameters. Therefore, we suppose that the model developed in these conditions will represent all of the experimental data. In the NN model, the performance of training set was computed in 3500 iterations as 8.116×10^{-4}, and the performance of testing set was computed as 8.841×10^{-4} (see Fig. 6).

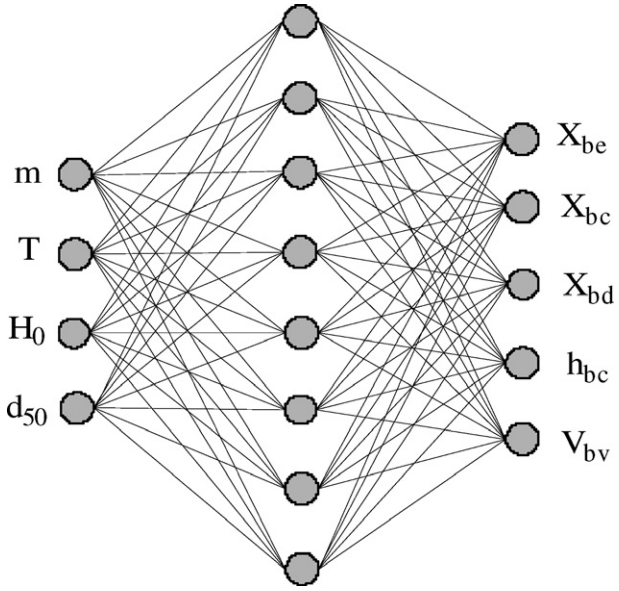


Fig. 5. The architecture of NN.

4.3. Explicit formulation of the NN model

Although NN was employed successfully to solve complex engineering problems, its capacity to establish a functional relationship between input and output data was not thoroughly investigated [49]. The functional relationship between input parameters and the output parameters was derived based on the trained NN model. The bar parameters were obtained in the functional form as:

$$X_{be} = \frac{13.6}{1 + e^{-(F_1 - 9.1206)}} \tag{17}$$

$$X_{bc} = \frac{13.6}{1 + e^{-(F_2 + 1.2078)}} \tag{18}$$

Table 3
Performance measures for various training/testing sets of NN model.

Training%:testing%	Training set performance		Testing set performance	
	MSE × 10^{-4}	R^2	MSE × 10^{-4}	R^2
80:20	8.116	0.979	8.841	0.980
70:30	8.18	0.977	9.412	0.979
60:40	7.71	0.979	11.890	0.972
50:50	7.40	0.980	13.260	0.964

Table 4
Experiment conditions and scenarios.

Exp. no	m	T (s)	H_0 (m)	d_{50} (m)	Exp. no	m	T (s)	H_0 (m)	d_{50} (m)
01	0.1000	1.46	0.065	0.00018	41	0.0667	1.46	0.160	0.00018
02	0.1000	1.46	0.065	0.00026	42	0.0667	1.46	0.160	0.00026
03	0.1000	1.46	0.115	0.00018	**43**	**0.0667**	**1.46**	**0.160**	**0.00033**
04	0.1000	1.46	0.115	0.00026	44	0.0667	1.46	0.160	0.00040
05	**0.1000**	**1.46**	**0.115**	**0.00033**	45	0.0667	1.46	0.200	0.00018
06	0.1000	1.46	0.160	0.00018	46	0.0667	1.46	0.200	0.00026
07	**0.1000**	**1.46**	**0.160**	**0.00026**	47	0.0667	1.46	0.200	0.00040
08	0.1000	1.46	0.160	0.00033	**48**	**0.0667**	**1.46**	**0.230**	**0.00018**
09	0.1000	1.46	0.160	0.00040	49	0.0667	1.46	0.230	0.00026
10	**0.1000**	**1.46**	**0.200**	**0.00018**	50	0.0667	1.46	0.230	0.00033
11	0.1000	1.46	0.200	0.00026	51	0.0667	1.46	0.260	0.00026
12	0.1000	1.46	0.200	0.00033	**52**	**0.0667**	**1.46**	**0.260**	**0.00033**
13	0.1000	1.46	0.200	0.00040	53	0.0667	1.46	0.260	0.00040
14	0.1000	1.46	0.230	0.00018	**54**	**0.0667**	**1.46**	**0.300**	**0.00018**
15	0.1000	1.46	0.230	0.00026	55	0.0667	1.46	0.300	0.00026
16	0.1000	1.46	0.230	0.00033	56	0.0667	1.46	0.300	0.00033
17	**0.1000**	**1.46**	**0.230**	**0.00040**	57	0.0667	1.46	0.300	0.00040
18	0.1000	1.46	0.260	0.00018	58	0.0667	2.03	0.115	0.00026
19	0.1000	1.46	0.260	0.00026	59	0.0667	2.03	0.115	0.00033
20	0.1000	1.46	0.260	0.00033	60	0.0667	2.03	0.160	0.00018
21	0.1000	1.46	0.300	0.00018	**61**	**0.0667**	**2.03**	**0.160**	**0.00026**
22	0.1000	1.46	0.300	0.00026	62	0.0667	2.03	0.160	0.00033
23	**0.1000**	**1.46**	**0.300**	**0.00033**	63	0.0667	2.03	0.200	0.00018
24	0.1000	1.46	0.300	0.00040	**64**	**0.0667**	**2.03**	**0.200**	**0.00026**
25	0.1000	2.03	0.115	0.00018	65	0.0667	2.03	0.200	0.00033
26	0.1000	2.03	0.115	0.00026	**66**	**0.0400**	**1.46**	**0.065**	**0.00018**
27	0.1000	2.03	0.115	0.00033	67	0.0400	1.46	0.065	0.00026
28	0.1000	2.03	0.160	0.00018	68	0.0400	1.46	0.115	0.00018
29	**0.1000**	**2.03**	**0.160**	**0.00026**	69	0.0400	1.46	0.115	0.00026
30	0.1000	2.03	0.160	0.00033	70	0.0400	1.46	0.115	0.00033
31	0.1000	2.03	0.160	0.00040	71	0.0400	1.46	0.160	0.00018
32	0.1000	2.03	0.200	0.00018	72	0.0400	1.46	0.160	0.00026
33	0.1000	2.03	0.200	0.00026	73	0.0400	1.46	0.160	0.00033
34	0.1000	2.03	0.200	0.00033	74	0.0400	1.46	0.230	0.00026
35	0.1000	2.03	0.200	0.00040	**75**	**0.0400**	**1.46**	**0.230**	**0.00033**
36	0.0667	1.46	0.065	0.00018	76	0.0400	2.03	0.115	0.00018
37	0.0667	1.46	0.065	0.00026	77	0.0400	2.03	0.115	0.00026
38	0.0667	1.46	0.115	0.00018	**78**	**0.0400**	**2.03**	**0.160**	**0.00018**
39	**0.0667**	**1.46**	**0.115**	**0.00026**	79	0.0400	2.03	0.160	0.00026
40	0.0667	1.46	0.115	0.00033	80	0.0400	2.03	0.160	0.00033

Note: The bold experiment numbers represent 16 cases for testing set.

$$X_{bd} = \frac{13.6}{1 + e^{-(F_3 - 6.2828)}} \tag{19}$$

$$h_{bc} = \frac{0.5637}{1 + e^{-(F_4 - 1.0711)}} \tag{20}$$

$$V_{bv} = \frac{0.5637}{1 + e^{-(F_5 + 0.8054)}} \tag{21}$$

Three output parameters (X_{be}, X_{bc}, and X_{bd}) in Eqs. (17)–(19) were normalized with the maximum of values of these parameters while two output parameters (h_{bc} and V_{bv}) in Eqs. (20) and (21) were normalized with the maximum of values of these two parameters. The constants of 13.6 and 0.5637 show the values used for normalization. Bias values were also given in each formula in Eqs. (17)–(21). F is given in matrice form as below:

$$F^T = \{ F_1 \ F_2 \ F_3 \ F_4 \ F_5 \ F_6 \ F_7 \ F_8 \} \tag{22}$$

$$F = W_0 \cdot out_H \tag{23}$$

$$W_0 = \begin{bmatrix} 3.7286 & 1.1852 & 2.0034 & -2.3642 & 2.1546 & 1.0786 & 0.1957 & 3.7924 \\ 3.6902 & 0.9924 & 4.1506 & -0.6631 & 2.5593 & 4.7176 & 0.1593 & -8.2661 \\ 2.0820 & 0.6184 & 7.8782 & 3.1125 & 3.9824 & 3.6954 & 1.9211 & -1.2379 \\ 0.5061 & 2.3818 & 2.0828 & -0.6314 & 2.5888 & -2.1553 & -1.0335 & -3.5155 \\ -14.9238 & 7.1061 & -7.0415 & -4.0837 & 0.9514 & 2.6131 & -0.4429 & 9.0690 \end{bmatrix} \tag{24}$$

where W_0 given is the weight matrice of 8 neurons between the hidden layer and the output layer. out_H is the output vector of 8 neurons in the hidden layer, which is expressed as:

$$out_H^T = \left\{ \frac{1}{1+e^{-y_1}} \ \frac{1}{1+e^{-y_2}} \ \frac{1}{1+e^{-y_3}} \ \cdots \ \frac{1}{1+e^{-y_8}} \right\} \tag{25}$$

$$Y_H = W_H \cdot X + \theta_H \tag{26}$$

$$Y_H^T = \{ y_1 \ y_2 \ y_3 \ y_4 \ y_5 \ y_6 \ y_7 \ y_8 \} \tag{27}$$

Table 5
Number of data and percentage of each parameter value in the all of the experiment data and testing set.

Parameter	Value	In the all set (80 cases)		In testing set (16 cases)	
		Number of data	%	Number of data	%
	0.1000	35	43.7	6	37.5
	0.0667	30	37.5	7	43.7
	0.0400	15	18.8	3	18.8
	1.46	56	70.0	11	68.7
	2.03	24	30.0	5	31.3
H_0	0.065	6	7.5	1	6.2
	0.115	16	20.0	2	12.5
	0.160	21	26.3	5	31.3
	0.200	14	17.5	2	12.5
	0.230	9	11.3	3	18.8
	0.260	6	7.5	1	6.2
	0.300	8	10.0	2	12.5
d_{50}	0.00018	23	28.8	5	31.3
	0.00026	26	32.5	5	31.3
	0.00033	21	26.3	5	31.3
	0.00040	10	12.5	1	6.2

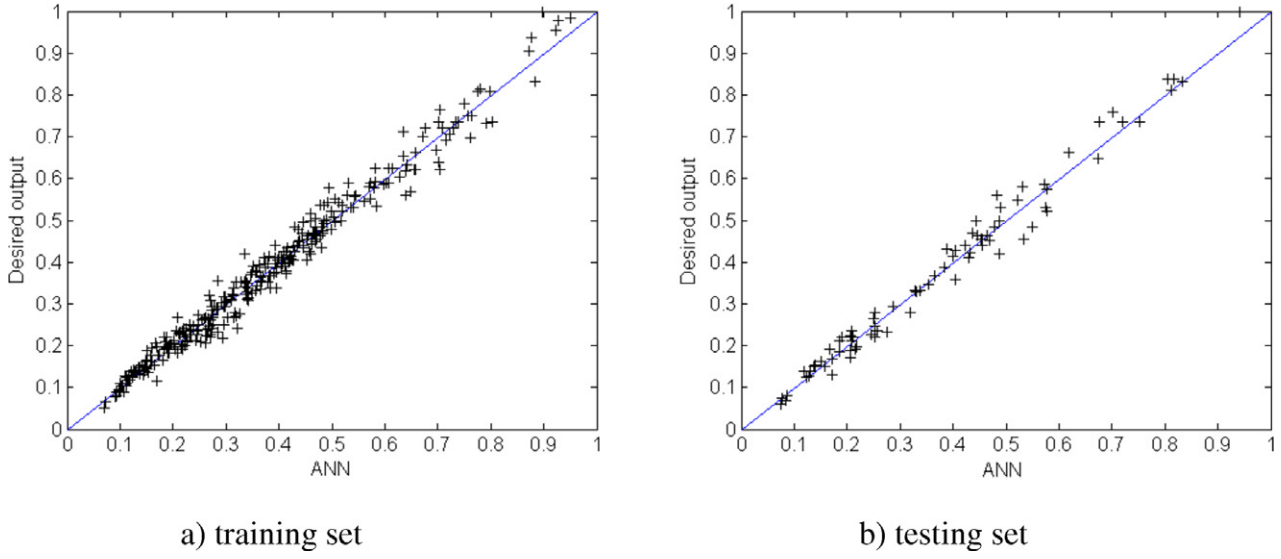


Fig. 6. The performance of NN for training and testing set.

$$W_H^T = \begin{bmatrix} -0.3502 & 0.8164 & -1.6028 & 3.2131 & -4.7671 & -4.6196 & -14.9207 & 1.8660 \\ 2.7726 & -2.4225 & -9.8762 & 5.2557 & 17.1963 & -7.3798 & 9.8829 & 4.3328 \\ -2.3899 & -2.7721 & 3.0847 & -5.0787 & 2.3179 & 2.9700 & 3.0191 & -4.5067 \\ 0.1920 & -5.8845 & -0.5741 & 1.0480 & -0.3071 & 2.3208 & -6.3148 & 7.1252 \end{bmatrix} \quad (28)$$

$$\theta_H^T = \{\, 1.1307 \;\; 11.2160 \;\; 6.8135 \;\; -4.2731 \;\; -13.6852 \;\; -5.0300 \;\; -0.5133 \;\; 5.2220 \,\} \quad (29)$$

$$X^T = \left\{ \frac{m}{0.1} \;\; \frac{T}{2.03} \;\; \frac{H_0}{0.3} \;\; \frac{d_{50}}{0.0004} \right\} \quad (30)$$

W_H and θ_H are the weight matrices and bias value vector of input variables in the input layer to neurons in the hidden layer. X is the normalized input vector. The values of denominators in Eq. (30) are the maximum values of each input parameters used for normalization.

Formulas of bar-shape parameters are valid within the values of Eq. (30).

4.4. Sensitivity analysis for input variables

The sensitivity analysis is carried out to investigate the effect of input parameters on the output results. The effect of changes in the input variables were the essence of the sensitivity analysis and it reflects the relative importance of each input variables. There are four input variables and five output variables in the established NN model in this study. Therefore, examination of the sensitivity analysis was carried out for 5 cases, which were established by excluding one of each input variables in each case. The results and cases were given in Table 6. According to Table 6, Case 1 gives the best results for both training and testing period. The most important parameter was observed as the slope, m, in Case 2 and deep water wave height, H_0, in Case 4.

Table 6
Five cases used in sensitivity analysis and results.

	Training set performance		Testing set performance	
	MSE × 10^{-4}	R^2	MSE × 10^{-4}	R^2
Case 1	8.116	0.979	8.841	0.980
Case 2	114	0.702	140	0.68
Case 3	39	0.899	53	0.879
Case 4	125	0.676	159	0.636
Case 5	22	0.943	27	0.938

Note: Case 1: ANN model ($m + T + H_0 + d_{50}$), Case 2: $T + H_0 + d_{50}$, Case 3: $m + H_0 + d_{50}$, Case 4: $m + T + d_{50}$, and Case 5: $m + T + H_0$.

5. Results and discussion

The performance of the NN model calibrated with part of the experimental data was compared to the performance of existing equations cited in literature. The NN model was also assessed with the best regression equations developed by utilizing from the experimental data used in the present study in reference [33]. The comparison is made in terms of relative error (e). The relative errors were calculated as in Eq. (31):

$$e = \left[\frac{x_m - x_c}{x_m}\right] \times 100 \tag{31}$$

where X_m and X_c are calculated and predicted (equations and NN) values, respectively. Average and standard deviation values of the relative errors were calculated and presented in Table 7. In this table, X_{bd} was determined by Eq. (4) and as $h_{bd}/\tan\beta$. Average errors for X_{be}, X_{bc}, X_{bd}, h_{bc}, and V_{bv} were obtained as 8.50%, 6.55%, 4.43%, 6.39%, and 6.38% for the NN model, respectively. As can be seen from this, NN model yielded the best results in comparison with the regression equations developed in the study of reference [33] and the literature equations for the entire bar-shape parameters, with min and max errors for X_{bd} (4.43%) and X_{be} (8.5%), respectively. Average error for NN was nearly 6.45%, which means this model can be evaluated as a more reliable one. There was a great difference between the values of NN and the literature equations while the performance of NN was slightly better than that of regression equations. The reliability of regression equations and the equations cited in literature was less than that of NN. The errors values of the literature equations for X_{be}, X_{bc} and h_{bc} were between 22 and 27%; however, for X_{bd} and V_{bv} showing great deviations (43–46%) while the regression equations have the errors values of 5% for X_{bd} and about 11% for other parameters. The reason for these deviations was supposed to be partly due to the fact that, the equations in the literature were based on less experimental data. Similar tendency was observed for the standard deviations of the errors.

Comparisons of the average error values of the NN, regression equations developed in the study of reference [33], equations cited in literature and experimental results are shown in Figs. 7–11. It is clear from these figures that equations cited in literature for X_{bd} and h_{bc} have a great difference in comparison with the experimental results. For these bar-shape parameters regression equations and the NN models have values close to each other for all the experimental numbers and they also have similar tendency with the experimental results. Values observed for the other experimental numbers except for experimental numbers 10, 48, and 54 were close to each other for V_{bv} in all the NN models, regression equations, and equations cited in literature. Equation cited in literature has too higher values than the experimental results in the experimental numbers 10, 48, and 54. Besides, results of the NN were much closer to the experimental results rather than that of regression equations and equations cited in literature for all of the experimental numbers for X_{be} and X_{bc}. They have slightly lower or higher values compared to the results of the NN. Finally, we concluded that the NN can be evaluated as a more reliable one compared to regression equations and equations cited in literature.

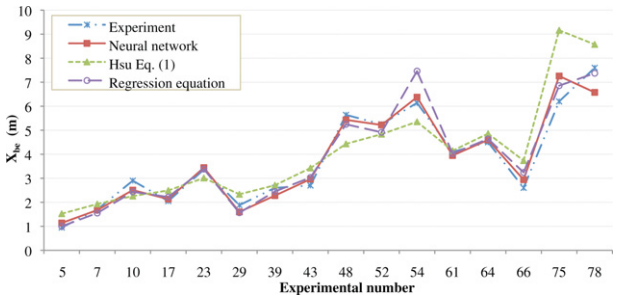


Fig. 7. Comparison of NN and regression and literature equations with test results for X_{be}.

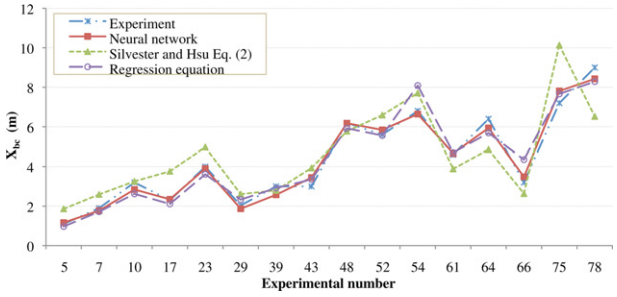


Fig. 8. Comparison of NN and regression and literature equations with test results for X_{bc}.

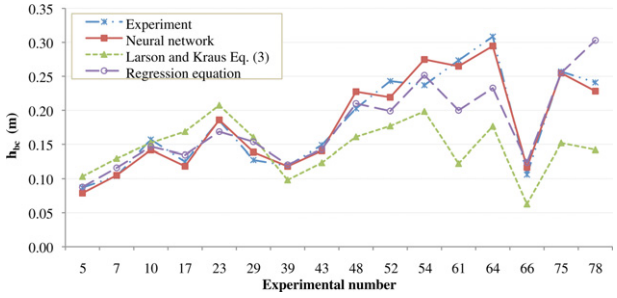


Fig. 9. Comparison of NN and regression and literature equations with test results for h_{bc}.

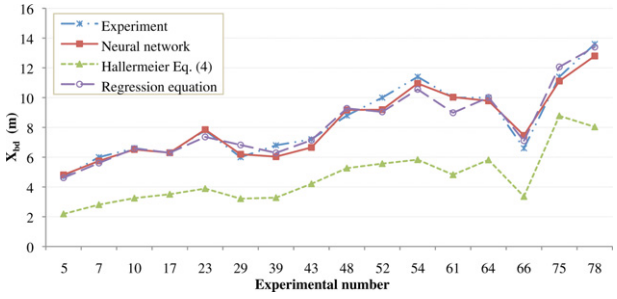


Fig. 10. Comparison of NN and regression and literature equations with test results for X_{bd}.

Table 7
Average and standard deviation values of the relative errors.

Parameters	Eq. type	Eq. number	Average error (%)	Standard deviation
$_{be}$	Neural network		8.50	6.35
	Hsu [10]	(1)	21.17	16.65
	Regression equation		9.48	7.08
X_{bc}	Neural network		6.55	4.37
	Silvester and Hsu [9]	(2)	26.56	18.96
	Regression equation		10.87	8.53
h_{bc}	Neural network		6.39	4.62
	Larson and Kraus [8]	(3)	27.43	13.91
	Regression equation		11.51	9.26
X_{bd}	Neural network		4.43	3.85
	Hallermeier [13]	(4)	45.71	7.58
	Regression equation		5.24	4.12
V_{bv}	Neural network		6.38	6.18
	Larson and Kraus [8]	(5)	43.81	51.09
	Regression equation		11.38	7.72

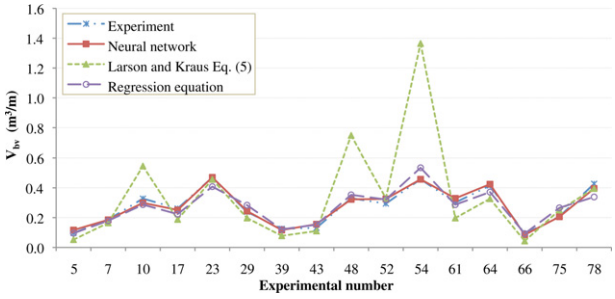


Fig. 11. Comparison of NN and regression and literature equations with test results for V_{bv}.

6. Conclusions

In this study, using 80 experiments, a neural network model (NN) was calibrated to predict bar-shape parameters of beach profiles. The performance of the NN model calibrated with part of the experimental data was compared to the performance of regression equations and existing equations cited in literature.

The results for X_{be}, X_{bc}, h_{bc}, X_{bd} and V_{bv} indicated that the NN fits to experimental data better than regression equations and existing equations cited in literature. In literature equations, the error values for X_{be}, X_{bc} and h_{bc} were less than those of X_{bd} and V_{bv}.

The use of NN model for experimental studies has begun recently in coastal and ocean engineering. Since the results of NN model are found to be satisfactory in this study, the usage of NN model in coastal and ocean engineering is encouraged and recommended for future studies.

References

[1] Dean RG. Physical modelling of littoral processes. In: RA Dalrymple (Ed.), Physical modelling in coastal engineering. New York: A.A. Balkema Uıtgevers B.V.; 1985, pp. 119–139.
[2] Kalra R, Deo MC, Kumar R, Agarwal VK. RBF network for spatial mapping of wave heights. Marine Structures. 2005;18:35–49.
[3] Lakhan VC, Trenhaile AS. Applications in coastal modelling. Amsterdam, The Netherlands: Elsevier Science B.V.; 1989.
[4] Zheng J, Dean RG. Numerical models and intercomparisons of beach profile evolution. Coastal Engineering. 1996;30:169–201.
[5] Leont'yev IO. Numerical modelling of beach erosion during storm event. Coastal Engineering. 1996;29:187–200.
[6] Larson M. Model of beach profile change under random waves. Journal of Waterway, Port, Coastal, and Ocean Engineering. 1996;122:172–181.
[7] Schoonees JS, Theron AK. Evaluation of 10 cross-shore sediment transport/morphological models. Coastal Engineering. 1995;25:1–41.
[8] Larson H, Kraus NC. Numerical model for simulating storm-induced beach change. Technical report, CERC-89–9, (SBEACH), Report 1. Empirical Foundation and Model Development, US Army Engineer Waterways Experiment Station, Coastal Engineering Research Center, Mississipi, USA; 1989.
[9] Silvester R, Hsu JRC. Coastal stabilization, advanced series on ocean engineering, Australia:. World Scientific Publishing; 1997.
[10] Hsu T-W. Geometric characteristics of storm-beach profiles caused by inclined waves. Ocean Engineering. 1998;25:69–84.
[11] Ruessink BG, Bell PS, Enckevort IMJ, Aarninkhof SGJ. Nearshore bar crest location quantified from time-averaged x-band radar images. Coastal Engineering. 2002;45:19–32.
[12] Günaydın K, Kabdaşlı MS. Investigation of offshore bar geometry under regular and irregular waves. Journal of Coastal Research. 2005;21:374–382.
[13] Hallermeier RJ. Uses for a calculated limit depth to beach erosion. In: 16th international conference on coastal engineering, ASCE. 1978, pp. 1493–1512.
[14] Deo MC, Naidu CS. Real time wave forecasting using neural networks. Ocean Engineering. 1999;26:191–203.
[15] Tsai CP, Lee TL. Back-propagation neural network in tidal level forecasting. Journal of Waterway, Port, Coastal, and Ocean Engineering. 1999:195–201.
[16] Deo MC, Jha A, Chapheker AS, Ravikant K. Neural network for wave forecasting. Ocean Engineering. 2001;28:889–898.
[17] Deo MC, Jagdale SS. Prediction of breaking waves with neural networks. Ocean Engineering. 2003;30:1163–1178.
[18] Huang W, Murray C, Kraus N, Rosati J. Development of a regional neural network for coastal water level prediction. Ocean Engineering. 2003;30:2275–2295.
[19] Altunkaynak A, Ozger M. Temporal significant wave height estimation from wind speed by perceptron Kalman filtering. Ocean Engineering. 2004;31:1245–1255.
[20] Makarynskyy O, Makarynska D, Kuhn M, Featherstone WE. Predicting sea level variation with artificial neural network at Hillarys Boat Harbour, Western Australia. Estuarine Coastal and Shelf Science. 2004;61:351–360.
[21] Balas CE, Koç L, Balas L. Predictions of missing wave data by recurrent neuronets. Journal of Waterway, Port, Coastal and Ocean Engineering. 2004;130:256–265.
[22] Tolman HL, Krasnopolsky VM, Chalikov DV. Neural network approximations for non-linear interactions in wind wave spectra: direct mapping for wind seas in deep water. Ocean Modelling. 2005;8:253–278.
[23] Kamphuis JW. On understanding scale effect in coastal mobile bed models. In: RA Dalrymple (Ed.), Physical modelling in coastal engineering. A.A. Balkema Uıtgevers B.V.; 1985, pp. 1141–1162.
[24] Yagcı O, Mercan DE, Cigizoglu HK, Kabdasli MS. Artificial intelligence methods in breakwater damage ratio estimation. Ocean Engineering. 2005;32:2088–2106.
[25] Ozger M, Sen Z. Prediction of wave parameters by fuzzy logic approach. Ocean Engineering. 2007;34:460–469.
[26] Ozger M. Significant wave height forecasting using wavelet fuzzy logic approach.

Ocean Engineering. 2010;37:1443–1451.
[27] Kankal M, Kömürcü Mİ, Yüksek Ö, Akpınar A. Artificial neural networks for estimations of temporal rate coefficient of equilibrium bar volume. Indian Journal of Geo-Marine Sciences. 2012;41:909–919.
[28] Kankal M, Yüksek Ö. Artificial neural network approach for assessing harbor tranquility: the case of Trabzon yacht harbor, Turkey. Applied Ocean Research. 2012;38:23–31.
[29] Larson M, Kraus NC, Wise RA. Equilibrium beach profiles under breaking and non-breaking waves. Coastal Engineering. 1999;36:59–85.
[30] Tihn NX. Modeling of coastal overwash. MD thesis. Lund, Sweden: Lund University, Lund Institute of Technology; 2006.
[31] USACE. Coastal engineering manual, engineer manual 1110–2–1100, vol. 3. Washington, DC: US Army Corps of Engineers; 2002.
[32] Kankal M, Kömürcü Mİ, Yüksek Ö, Akpınar A. Artificial neural networks for estimation of temporal rate coefficient of equilibrium bar volume. Indian Journal of Geo-Marine Sciences. 2012;41:909–919.
[33] Kömürcü Mİ, Özölçer İH, Yüksek Ö, Karasu S. Determination of bar parameters caused by cross-shore sediment movement. Ocean Engineering. 2006;34:685–695.
[34] Kömürcü Mİ, Yüksek Ö, Karasu S, Özölçer İH. An experimental study on bar characteristics of storm-built profiles. In: 6th International Conference on the Mediterranean Coastal Environment, MEDCOAST. 2003, pp. 1685–1693.
[35] U.S. Army Corps of Engineers. Coastal engineering manual. Engineer manual 1110_2-1100. Washington, DC: U.S. Army Corps of Engineers; 2002.
[36] Seelig WN, Ahrens JP. Estimation of wave reflection and energy dissipation for beaches, revetments, and breakwater. CERC technical paper 81–1. Vicksburg, MS: US Army Corps of Engineers Waterways Experiment Station; 1981.
[37] Smith ER. Potential toe scour and wave reflection at revetments. Miscellaneous paper CERC-96–2. Vicksburg, MS: US Army Corps of Engineers Waterways Experiment Station; 1996.
[38] Noda EK. Equilibrium beach profile scale-model relationship. Journal of Waterways, Harbours and Coastal Engineering Division-ASCE. 1972:511–527.
[39] Ito M, Tsuchiya Y. Scale-model relationship of beach profile. In: 19th coastal engineering conference, ASCE. 1984, pp. 1386–1402.
[40] Wang X, Lin LH, Wang H. Scaling effects on beach response physical model. In: 24th coastal engineering conference, ASCE. 1994.
[41] Kömürcü Mİ. Determination of bar parameters caused by cross-shore sediment movement. PhD thesis. Trabzon, Turkey: Karadeniz Technical University Natural and Applied Sciences Institute; 2004 [in Turkish].
[42] Kömürcü Mİ, Tutkun T, Özölçer İH, Akpınar A. Estimation of the beach bar parameters using the genetic algorithms. Applied Mathematics and Computation. 2008;195:49–60.
[43] Rao VB. C++ neural networks and fuzzy logic. M&T Books; 1995.
[44] Rumelhart DE, MacClelland JL. Parallel distributed processing: explorations in the microstructure of cognition. Cambridge, MA: MIT Press; 1986.
[45] Kasabov NK. Foundations of neural networks, fuzzy systems, and knowledge engineering, London, England:. Cambridge, MA: MIT Press; 1996.
[46] Haykin S. Neural networks: a comprehensive foundation. New Jersey: Prentice-Hall; 1994.
[47] Freeman JA, Skapura DM. Neural networks algorithms, applications, and programming techniques. Addison-Wesley Pub.; 1991.
[48] Moller MF. A scaled conjugate gradient algorithm for fast supervised learning. Neural Networks. 1993;6:525–533.
[49] Pu Y, Mesbahi E. Application of artificial neural networks to evaluation of ultimate strength of steel panels. Engineering Structures. 2006;28:1190–1196.